NIPES

Advances in Engineering Design Technology

Journal homepage: www.nipesjournals.org.ng

Experimental and Numerical Optimization of Tungsten Inert Gas (TIG) Welding Process Parameters Relative to Mechanical Properties of AISI 1018 Mild Steel Plate

Owunna Ikechukwu Bismarck*, Ikpe Aniekan Essienubong

Department of Mechanical Engineering, University of Benin, Benin City, Edo State, PMB 1154, Nigeria

ARTICLE INFORMATION

Keywords:
Welding parameters, Welding experiment, Numerical optimization, Mechanical properties, Welded joint

Received 28 Oct. 2021
Revised 22 November 2021
Accepted 25 November 2021
Available online 19 January 2022

https://doi.org/10.37933/nipes.a/3.2.2021.11

https://nipesjournals.org.ng

ABSTRACT

In this study, central composite design (CCD) in Design Expert 7.01 software was used to generate statistical design of experiment (DOE) which is an acceptable design approach in Response Surface Methodology (RSM). Based on the DOE, an experimental design matrix having six centre points, six axial points and eight factorial points resulting in twenty experimental welding runs were generated as input parameters for experimental TIG welding process and numerical solution using RSM prediction and optimization. Requirements for the twenty experimental input welding runs were maximum UTS, maximum yield strength, minimum strain and minimum elongation, and welding run No. 8 met the requirement with the following welding input parameters: 210 amp current, voltage of 21.00 V, gas flow rate of 19.00 litters/min and welding speed of 3.75 mm/min. Significant correlations were observed in the four output results (UTS, yield strength, strain and elongation) obtained from the control sample, RSM predicted and experimentally determined results. The solution was selected by design expert as the optimal solution with a desirability value of 97.29%. Comparing the output results obtained from the control samples, welding experiment and RSM predicted values, significant correlations were observed in RSM predicted and experimentally determined welding results than that of the controlled samples. From the tensile test results obtained, the UTS and yield strength were observed to decrease as the applied force increased while the strain and elongation increased in the same trend with the applied force. Results from RSM and the control samples followed similar trends.

1. Introduction

Welding involves the process of joining two pieces of metal together by the application of intense heat, pressure or both to melt the weld region of the metals in order to fuse permanently [1]. In other words, a non-consumable tungsten electrode is applied in the fusion of two or more metals through a localized application of heat and its dissipation through conduction into the parent metal [2]. Welding processes is commonly used in joining sheet metals [3], the heat is produced after electrical energy has been converted to light energy which passes through the flux to the electrode to strike an arc, and the light energy is converted to heat energy which enables the welding operation. A welded joint is obtained when two clean surfaces are brought into contact with one other and either pressure or heat, or both are applied to obtain a bond. Tungsten Inert Gas (TIG) also referred to as

Gas Tungsten Arc Welding (GTAW) is a welding process that is often used for joining similar and dissimilar materials, and are more suitable for welding metals and their alloys [4]. TIG welding process involves the use of non-consumable tungsten electrodes such as EWTh-2, EWZR-1, EWLa-2, EWLa-1.5, EWLa-1, EWCe-2, EWP, to produce an arc and a filler wire to join the desired metals together while simultaneously shielding the welding environment with inert gas such as helium or argon to protect the molten weld pool from atmospheric contaminants [5]. Weld region surrounding the fusion line is known as the Heat Affected Zone (HAZ), which it is not completely heated to cause melting but is however affected by thermal heat during the welding process [6]. In recent time, studies have shown that heat distribution around the fusion zone can alter the chemical and mechanical properties of the weld which may depend upon the chemical composition of the bead and its geometry [7]. HAZ in steels can be sub-divided into the following zones depending on the highest welding temperature attained by the arc heat welding process: Under Bead Zone i.e., that part of HAZ which may be heated beyond the critical temperature of grain growth and extend up to the fusion boundary zone, Grain Growth Zone, beyond 1150^{o}C to peritectic temperature, Grain Refined Zone, 950 to 1150^{o}C, i.e., beyond A3 up to grain refined temperature range, Partially Transformed Zone, 750 to 950^{o}C, i.e., between A1 and A3 temperature, Zone of Spherodized Carbides, 550 to 750^{o}C, i.e., below A1, Zone of Unchanged Base Material, up to 550^{o}C [8].

The effect of electric power arc inputs on mechanical properties of 0.4%C steel by varying the currents from 100A for low heat input, 112.5A for medium heat input and 125A for high heat input was investigated [9]. Results indicated that increasing the welding current from 100A-125A caused a corresponding decrease in mechanical properties and an increase in brittleness of the specimens. The joints made by using low heat input exhibited higher tensile strength (515.90 Mpa), and from Scanning Electron Microscopy (SEM) of the tensile test, fractured surface exhibited ductile failure, higher hardness strength (179.5 HRC) and impact toughness value (6.5 Joules) than those welded with medium and high heat inputs which exhibited brittle failure as the heat inputs increased.

A range of TIG welding temperatures including 1746^{o}C, 1912^{o}C, 2100^{o}C, 2410^{o}C and 2800^{o}C was employed in the joining process of AISI 1020 low carbon steel plate of 10 mm thickness [10]. A strain gauge indicator was used to measure the thermal stresses induced on the steel plate which the average was recorded as 38,200MPa. The experimental parameters and conditions were applied in finite element simulation of the same plate dimension, and average von-mises stress of 37,508 MPa, average axial stress of 30,732 MPa and average thermal stress of 20,101 MPa were obtained. In addition, it was observed that the higher the welding temperature, the higher the stresses induced on the welding material.

Statistical design of experiment (DOE) using the central composite design method (CCD) was adopted to generate DOE for twenty (20) experimental runs as input variables (current, voltage and gas flowrate) and output responses (maximum UTS and maximum modulus of elasticity with corresponding elongation and strain) [11]. Artificial Neural Network (ANN) optimization approach was also used in predicting and optimizing the DOE generated. There was correlation between the experimental, ANN predicted and the observed values. Visuals of the weldment obtained from Scanning Electron Microscopy with Energy Dispersive Spectroscopy (SEM/EDS) revealed a uniformly distributed grain sizes in the weldment primarily composing of iron (Fe), chromium (Cr), molybdenum (Mo), and nickel (Ni).

Welding parameters including temperature ranging from 96.13-213.86 A, voltage ranging from 16.95-27.04 V and gas flow rate ranging from 11.29-19.70 L/min were employed as input for TIG welding experimental procedure as well as prediction and optimization using Response Surface Methodology (RSM) [12]. The output responses were temperature distribution, Induced Stress Distribution (ISD) and bead penetration depth. The optimized results revealed that input current of 120 A, voltage of 23.95 V and gas flow rate of 15.63 L/min can produce a weld joint with temperature of 326.53^{o}C, ISD of 231.746 N/m^{2} and bead penetration depth of 6.47911 mm. To validate the results, regression plot between the experimental values and RSM predicted values

showed proximity in the coefficient of determination (R^2) for the output responses which were close to 1.

Structural failure resulting from deterioration of weld quality has been a major problem in the manufacturing sector. Most of these failures occur at welded joints, which can be influenced by poor combination of the weld input parameters. Studies have shown that one of the practical approaches in improving weld qualities is to select optimum input process parameters, which can be achieved by adopting appropriate mathematical models. Hence, necessitating investigation on the effects of Tungsten Inert Gas (TIG) welding parameters on mechanical properties of AISI 1018 material using experimental and numerical optimization approach.

2. Materials and Method

The specific objectives of the optimization approach were to maximize the yield strength of TIG welds, maximize the UTS, minimized the strain and also to minimize the elongation. The final solution of the optimization process was to determine optimum values of the input variables (current, voltage, gas flow rate and welding speed) that can maximize yield strength, maximize UTS, minimize strain and minimize elongation property on the welds. The randomized design matrix comprised of four input variables namely: current (Amp), voltage (V), gas flow rate (L/min) and welding speed, with four output response variables, namely: yield strength, ultimate tensile strength, strain and elongation. To generate an experimental data for the optimization process, the following steps were adopted:

i. Statistical design of experiment (DOE) using the central composite design method (CCD) was done. Central composite design (CCD) is unarguably the most acceptable design for response surface methodology (RSM) [13]. The design and optimization was done using statistical software and for this particular problem, Design Expert 7.01 was employed.
ii. Design Expert 7.01 software was used to generate the design of experiment (DOE) for twenty (20) (having six centre points, six axial points and eight factorial points) experimental runs (see Table 1) as input parameters for experimental TIG welding procedure and RSM prediction and optimization.

Table 1: Welding Parameters from design of experiment

Weld Runs	Current (amps)	Voltage (V)	Gas flow rate (litters/min)	Welding speed (mm/min)
1	**180**	**21.00**	**19.00**	**3.75**
2	183	18.00	19.00	3.75
3	185	18.50	19.00	3.75
4	190	19.00	19.00	3.75
5	195	21.50	19.00	3.75
6	200	20.00	19.00	3.75
7	205	20.50	19.00	3.75
8	**210**	**21.00**	**19.00**	**3.75**
9	213	18.00	19.00	3.75
10	215	18.50	19.00	3.75
11	218	19.00	19.00	3.75
12	221	21.50	19.00	3.75
13	225	20.00	19.00	3.75

14	225	20.50	19.00	3.75
15	**240**	**21.00**	**19.00**	**3.75**
16	228	18.00	19.00	3.75
17	230	18.50	19.00	3.75
18	230	19.00	19.00	3.75
19	235	21.50	19.00	3.75
20	225	20.00	19.00	3.75

AISI 1018 is a mild/low carbon steel with carbon composition ranging from 0.14-0.20%, 98.81-99.26% of iron, 0.60-0.90% of manganese, ≤0.040% of phosphorous, ≤0.050% of Sulphur etc. [14], and has excellent weldability. It can be welded instantly by several conventional welding methods, and produces a uniform harder case which is the reason why it is considered one of the best steel materials for carburized parts [15], but welding of AISI 1018 steel is however not recommended when it is carbonnitrided. It offers a good balance of toughness, strength and ductility, and can be welded with low carbon welding electrode without post-heating and pre-heating.

AIS1 1018 low carbon steel plate of 10 mm thickness purchased from the local market was cut into a dimension of 120x30 mm (length x width) each. Emery paper was used to smoothen each of the two specimen to eliminate all possible coatings, corrosion or rust that may have accumulated on the material. The two steel plates were chamfered at 30 degrees, after which, fusion welding was used to join the two plates together to form an angle of 60 degrees with 2mm depth. Prior to welding, surface of the samples to be welded were chemically cleaned with acetone to eliminate surface contamination and welding was applied on the flat plates to fill the chamfered V-groove using the welding parameters in Table 1.

The welding torch passed over the plate at a height of 2.5mm from the workpiece at constant velocity of 1.72 mm/s^{-1}. After welding, surface of the 10 mm flat plates were prepared again through grinding, degreasing, abrading, conditioning and neutralizing. Grinding was done with the help of a grinding machine to remove spatters from the surface of the plate, degreasing was done by using GC-6 Isopropyl alcohol and gauze sponge to clean the surface of the beam in order to remove oil, grease and other contaminants from the surface of the metal plate. The surface was then wetted with mild acidic solution and then abraded again using a smooth emery paper to remove any other scales and oxides found on the surface of the plate. The application of mild acidic solution was to enhance the cleaning process. After abrading, the surface was again cleaned with gauze sponge and alcohol. A basic solution (M-pep neutralizer 5A) was then applied to neutralize the surface after which the surface was dried with gauze sponge. This procedure was repeated for 20 pieces of 10 mm flat steel plates which were now ready to be subjected to tensile testing.

Strain gauge rosette was attached on the weldment, with lead wires soldered on it while the other ends were connected to the input terminals (channels) of P3 Strain Indicator. A transparent glass shield was used to shield off the INSTRON machine to prevent the specimen from hitting anyone should it accidentally go of the machine during the test. The INSTRON tensile machine was switched on, the gauge meter were reset to zero to ensure the equipment does not display wrong data and forces ranging from 12,000-20,000 N were applied gradually on the flat plate. The twenty flat plate specimens were mounted on the instron tensile test machine and subjected to tensile test. The experimentation was carried out with the instron machine to record yield strength of the materials, Ultimate Tensile Strength (UTS) and strain values resulting from deformation as shown in Figure 1. Also, Figure 2 shows the twenty (20) best samples after the tensile test experimental procedure.

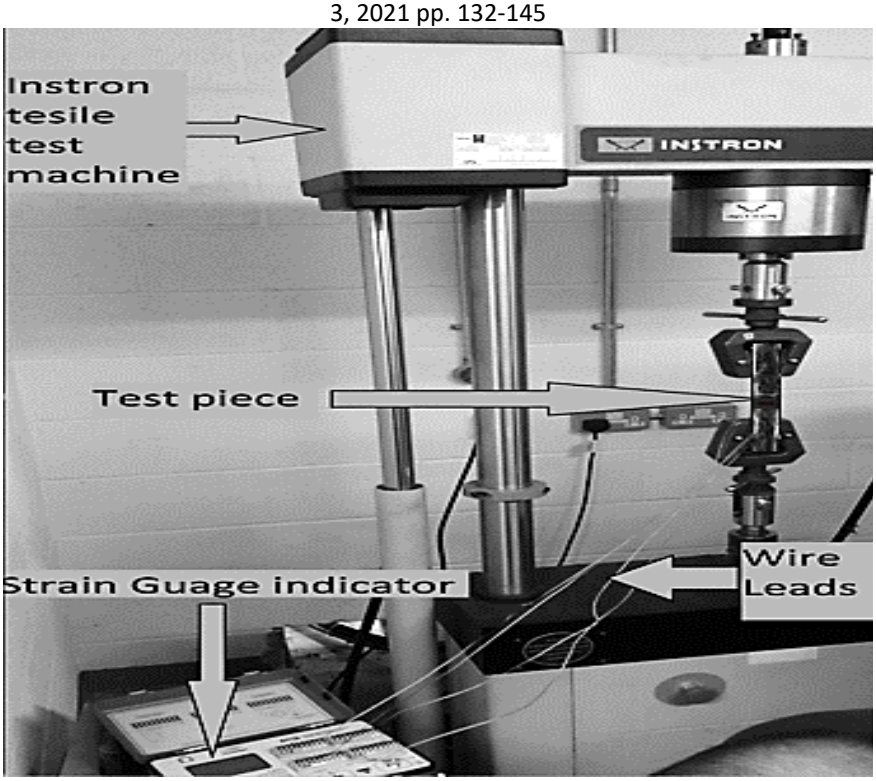

Figure 1: Experimental set-up for specimen mounted on instron tensile test machine

Figure 2: Test samples that have undergone tensile test from instron tensile test machine

3. Results and Discussion

Having obtained the results for twenty welding runs, numerical optimization was performed to ascertain the desirability of the overall model. In the numerical optimization phase, design expert was programmed to optimize these welding parameters (current, voltage, gas flow rate and welding speed). The optimized input welding parameters required for optimum output response were

tabulated in Table 2. From the numerical optimization, three welding runs (welding run number 1, 8 and 15) met the requirements with maximum yield strength, maximum UTS, minimum strain and minimum percentage elongation, and were applied as input variables in both welding experiment and RSM. Applying the optimized welding input variables or parameters experimentally, output responses or results for the three (3) welding runs were tabulated in Table 3-5 and graphically presented in Figure 3 and 4.

Table 2: Optimized welding parameters from design of experiment

Welding Runs	Current	Voltage	Gas Flow Rate	Welding Speed	Requirements
1	180	21.00	19.00	3.75	Maximum UTS, maximum yield strength, minimum strain and minimum elongation
8	210	21.00	19.00	3.75	
15	240	21.00	19.00	3.75	

Table 3: Results for Number 1 experimental welding Run

Sample	Force (N)	UTS (MPa)	Yield Strength (MPa)	Strain (e)	Elongation (%)
1	12000	448.612	363.718	0.19	19
2	12400	445.152	359.307	0.24	24
3	12700	441.468	355.415	0.27	27
4	13200	439.670	353.424	0.30	30
5	13500	437.265	351.840	0.31	31
6	13800	435.232	347.632	0.33	33
7	14200	432.256	345.167	0.36	36
8	14600	429.624	342.913	0.38	38
9	15000	425.313	339.326	0.40	40
10	15400	424.549	336.622	0.42	42
11	15700	420.378	332.705	0.43	43
12	16100	417.202	331.415	0.45	45
13	16500	415.563	328.712	0.47	47
14	16800	412.314	325.163	0.50	50
15	17200	409.432	323.674	0.52	52
16	17500	405.738	318.208	0.54	54
17	17900	403.624	317.350	0.56	56
18	18400	398.306	315.482	0.58	58
19	18700	395.43	311.126	0.60	60
20	19200	392.603	307.264	0.61	61

Table 4: Results for number 8 experimental welding Run

Sample	Force (N)	UTS (MPa)	Yield Strength (MPa)	Strain (e)	Elongation (%)
1	12000	497.981	398.519	0.16	16
2	12400	493.323	395.246	0.23	23

3	12700	489.764	391.910	0.27	27
4	13200	484.563	388.212	0.29	29
5	13500	481.387	382.853	0.30	30
6	13800	475.634	376.431	0.32	32
7	14200	472.958	369.372	0.35	35
8	14600	468.961	364.470	0.37	37
9	15000	453.842	360.236	0.39	39
10	15400	449.545	355.521	0.41	41
11	15700	444.676	353.243	0.42	42
12	16100	441.809	351.342	0.44	44
13	16500	436.673	349.473	0.45	45
14	16800	429.870	345.975	0.50	50
15	17200	425.458	342.763	0.51	51
16	17500	421.865	340.562	0.52	52
17	17900	417.913	337.241	0.53	53
18	18400	414.513	335.985	0.55	55
19	18700	411.208	333.247	0.57	57
20	19200	409.103	329.764	0.60	60

Table 5: Results for number 15 experimental welding Run

Sample	**Force (N)**	**UTS (MPa)**	**Yield Strength (MPa)**	**Strain (e)**	**Elongation (%)**
1	12000	470.203	372.614	0.21	21
2	12400	467.120	369.506	0.25	25
3	12700	465.324	366.312	0.29	29
4	13200	463.472	364.413	0.32	32
5	13500	459.368	360.943	0.35	35
6	13800	455.136	358.736	0.37	37
7	14200	452.354	355.174	0.40	40
8	14600	448.321	352.353	0.44	44
9	15000	443.243	350.216	0.45	45
10	15400	439.744	347.420	0.47	47
11	15700	435.572	345.446	0.50	50
12	16100	432.601	343.242	0.52	52
13	16500	430.376	341.371	0.56	56
14	16800	426.272	337.265	0.59	59
15	17200	423.408	334.573	0.63	63
16	17500	419.832	332.103	0.65	65
17	17900	414.703	330.140	0.66	66
18	18400	412.314	328.685	0.69	69
19	18700	409.258	323.209	0.73	73
20	19200	407.863	322.363	0.75	75

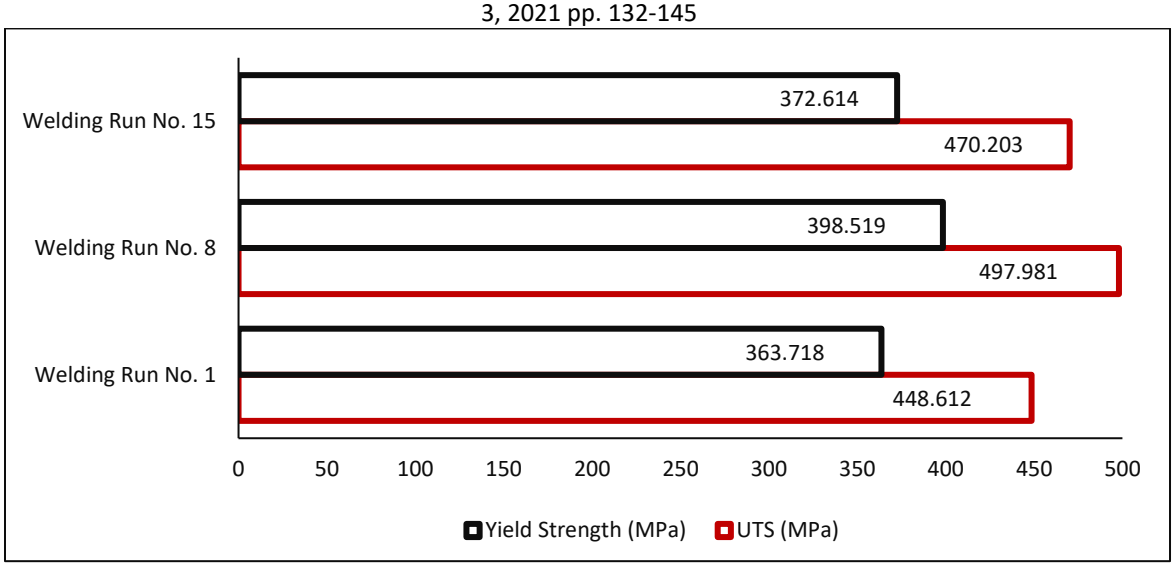

Figure 3: Plot of yield strength and UTS for selected winding runs

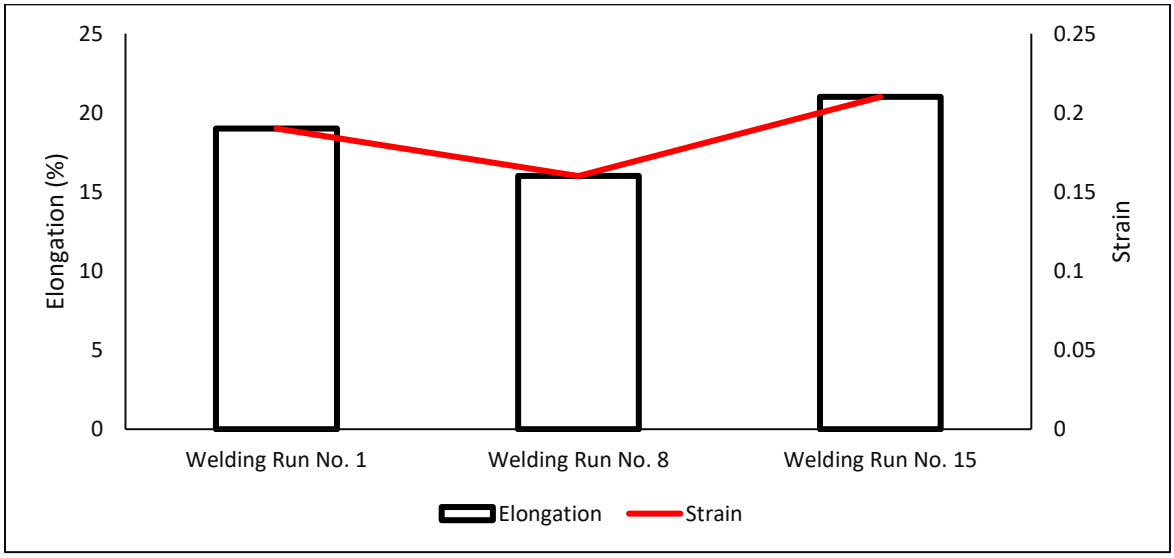

Figure 4: Plot of elongation and strain for selected winding runs

Considering the aforementioned constrains (maximum yield strength, maximum UTS, minimum strain and minimum percentage elongation) it is clear that results for number 8 welding run met the criteria, and was applied in RSM to predict the output responses. Applying the optimized welding input variables obtained from welding run No. 8, the output responses obtained were graphically presented in 3D plots as shown in Figures 5-8. To study the effects of combine variables on each responses, the 3D surface plot presented in Figures 5-8 were employed. Three dimensional surface plots were employed to give a clearer concept of the surface response. The presence of a colored hole at the middle of the upper surface gave a clue that more points lightly shaded for easier identification fell below the surface. The 3D surface plots as observed in Figures 5-8 indicated the relationship between the welding input variables (current, voltage, gas flow rate and welding speed) and output responses (yield strength, UTS, strain and elongation).

The sequential model sum of squares indicated the accumulating improvement in the model fit as terms are added. Based on the calculated sequential model sum of square, the highest order polynomial where the additional terms are significant and the model was not aliased was selected as the best fit. It was observed that the cubic polynomial was aliased, hence, cannot be employed to fit the final model. In addition, the quadratic and two-factor integration (2FI) models were suggested

as the best fit, thus justifying the use of quadratic polynomial in the analysis. To test how well the quadratic model can explain the underlying variations associated with the experimental data, lack of fit test was estimated for each response. While a model with significant lack of fit cannot be employed for prediction, non-significant lack of fit is good, as it indicates a model that is significant [12]. Based on the simulation outcome, the quadratic polynomial model was suggested while the cubic polynomial model was aliased, thus, the quadratic polynomial model was selected for this analysis. Analysis of the model standard error was employed to assess the suitability of response surface methodology using the quadratic model to maximize yield strength, maximize UTS, minimize strain and minimize percentage elongation of AISI 1018 mild steel plate. Analysis of variance (ANOVA) was used to check whether or not the model is significant and also to evaluate the significant contributions of individual variable, the combined and quadratic effects towards each response. ANOVA was employed in optimization of weld strength properties of TIG welding, which uses the variance of the group means (F-values) and probability of obtaining a result as significant as the one observed (P-value) [16]. To validate the adequacy of the quadratic model based on its ability to maximize yield strength, maximize UTS, minimize strain and minimize percentage elongation, goodness of fit statistics was employed. To obtain the optimal solution, the coefficient statistics and the corresponding standard errors were first considered. The computed standard error measures the difference between the experimental terms and the corresponding predicted terms.

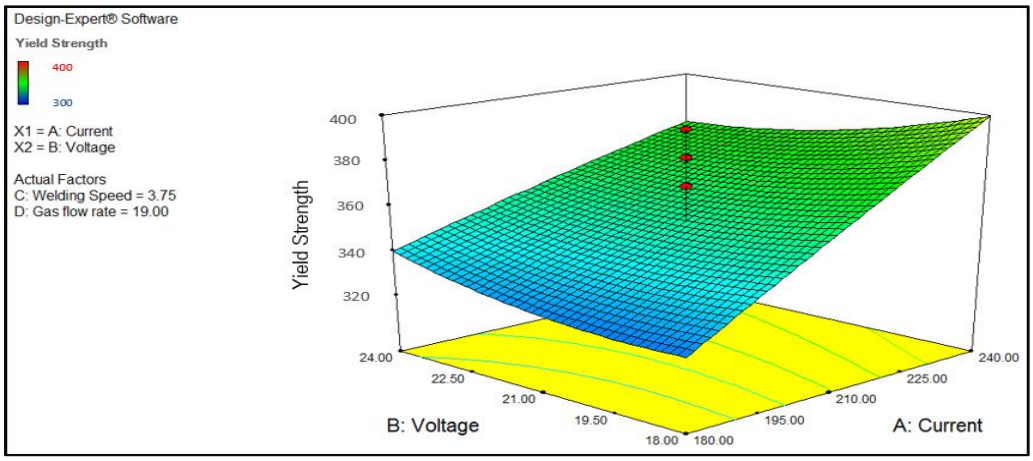

Figure 5: 3D plot of yield strength varying arc voltage and current for welding run No. 8

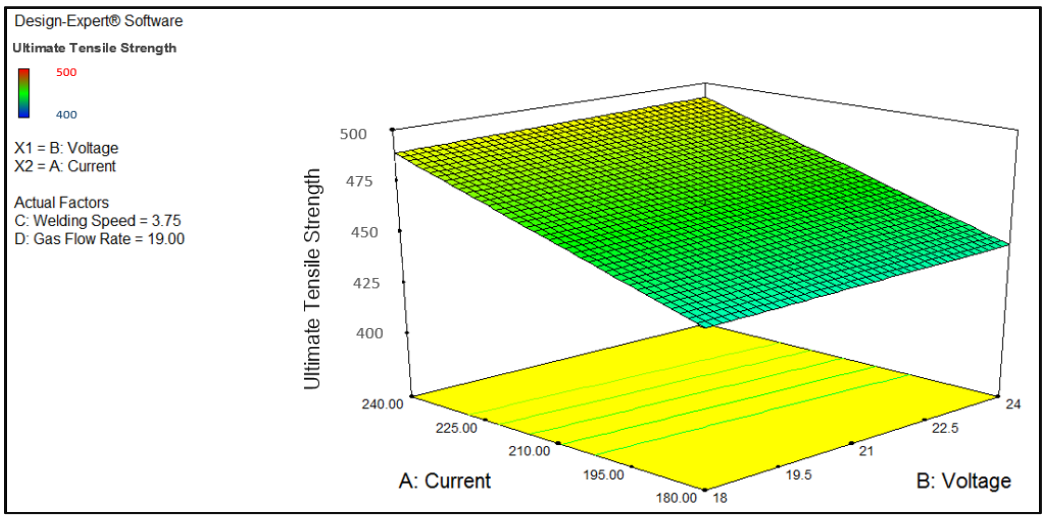

Figure 6: 3D plot of ultimate tensile strength varying welding current and arc voltage for welding run No. 8

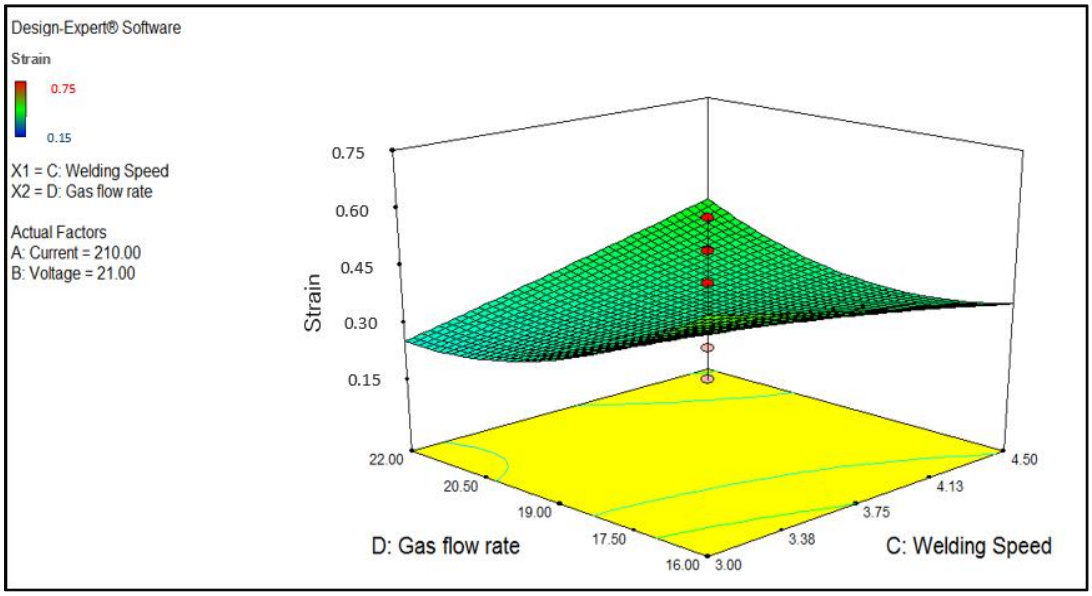

Figure 7: 3D plot of strain varying gas flow rate and welding speed for welding run No. 8

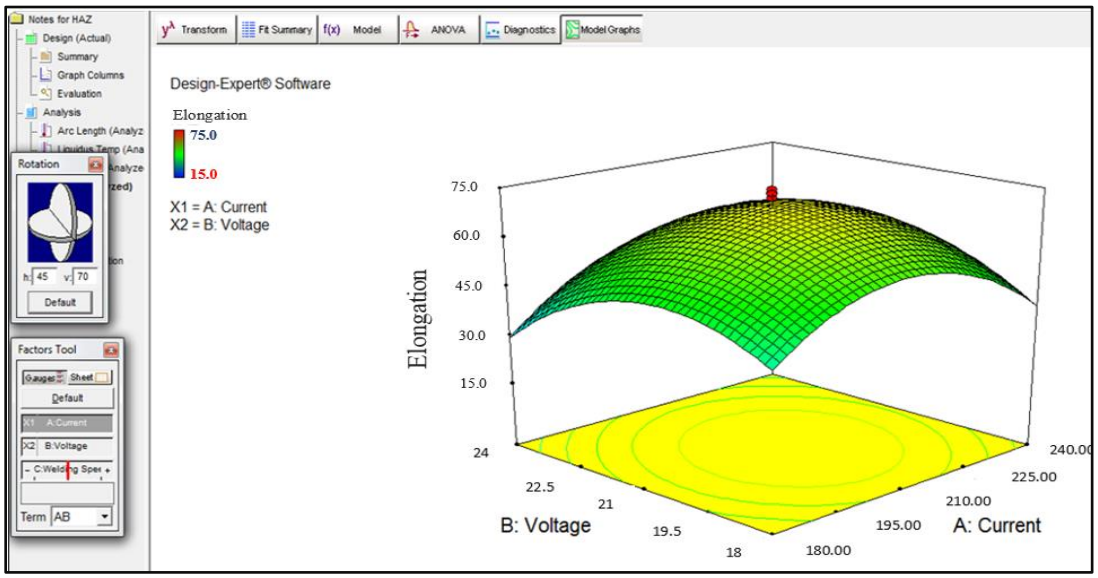

Figure 8: 3D plot of elongation varying arc voltage and welding current for welding run No. 8

The desirability bar chart which shows the accuracy with which the model is able to predict the values of the selected input variables and the corresponding responses is presented in Figure 9. It can be deduced from the result of Figure 9 that the model developed based on response surface methodology and optimized using numerical optimization method, predicted the output responses with the following accuracies:

i. UTS with an accuracy level of 98.22%
ii. Yield strength with an accuracy level of 97.10%
iii. Strain with an accuracy level of 96.55%
iv. Elongation with an accuracy level of 97.29%

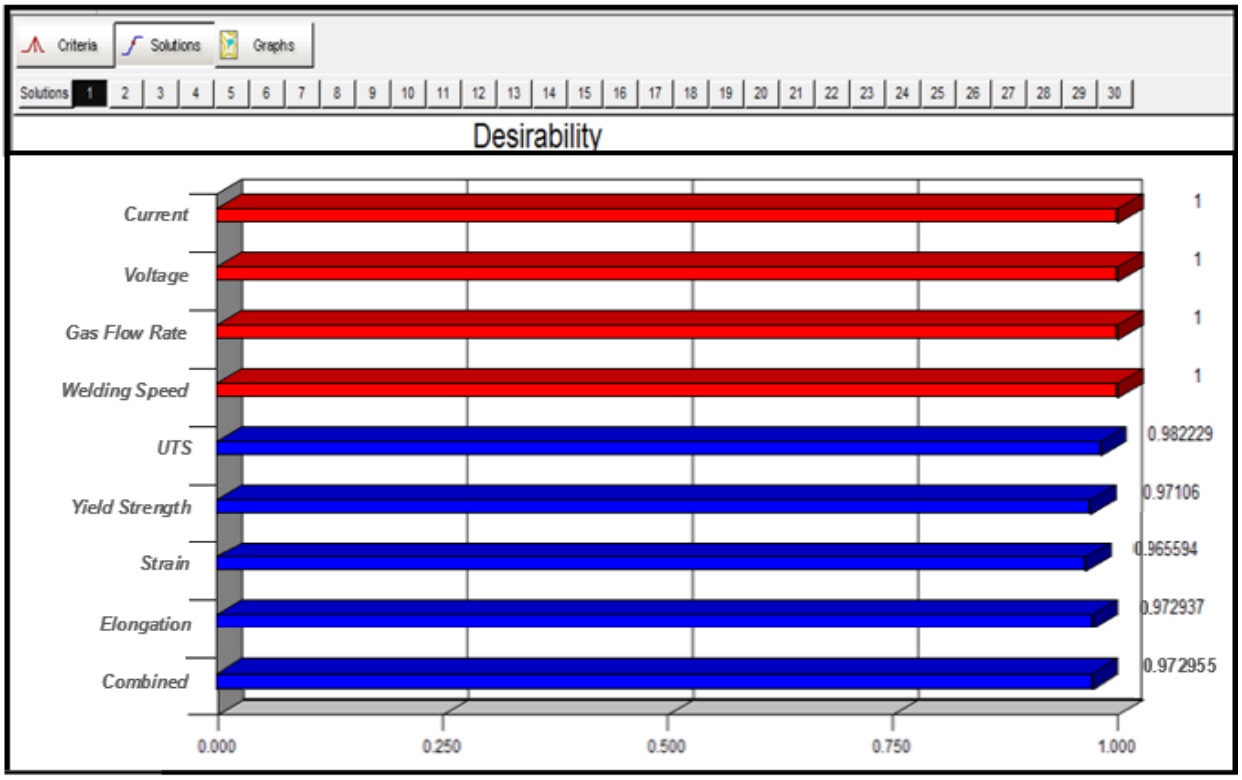

Figure 9: Prediction accuracy of numerical optimization with RSM

Combined value from the desirability plot was derived from the summation of the four output responses (UTS of 0.9822 accuracy + yield strength of 0.9710 accuracy + equivalent strain of 0.9655 accuracy + percentage elongation of 0.9729) divided by 4, making it 0.9729 which in percentage was expressed as 97.29% accuracy. In other words, calculating mean value from the four output responses predicted by RSM and multiplying by 100 to obtain the percentage accuracy. In a similar study where RSM was also adopted as the method for optimizing TIG welding parameters, desirability value of 95.70% was obtained [17] while desirability value of 97.30% was obtained in another study [18]. The aforementioned level of desirability which is almost 100% is an indication that RSM is an effective method for predicting and optimizing welding parameters for industrial applications [19, 20].

Figure 10 indicates the optimum welding process parameters with the control sample, RSM predicted values and experimental welding run No. 8 which represents the plot of UTS, yield strength, strain and elongation output results. From the plot, UTS values of 497.981MPa was experimentally obtained from the welded sample, 500MPa from RSM predicted result and 450 MPa from the control sample which were all computed using optimized welding parameters from weld run No. 8. Similarly, yield strength values of 398.519MPa was experimentally obtained from the welded sample, 400MPa from RSM predicted result and 380 MPa from the control sample which were all computed using optimized welding parameters from weld run No. 8. Furthermore, strain values of 16 was experimentally obtained from the welded sample, 15 from RSM predicted result and 15 from the control sample which were all computed using optimized welding parameters from weld run No. 8. In this context, strain (often considered a dimensionless parameter) is defined as the level of deformation experienced by AISI 1018 metal samples investigated in this study under the influence of applied load/force divided by the original dimension of the samples [21]. Finally, elongation values of 0.16% was experimentally obtained from the welded sample, 0.15% from RSM

predicted result and 0.15% from the control sample which were all computed using optimized welding parameters from weld run No. 8. Comparing the output results obtained from the control samples, welding experiment and RSM predicted values, significant correlations were observed in RSM predicted and experimentally determined welding results than those for the controlled samples.

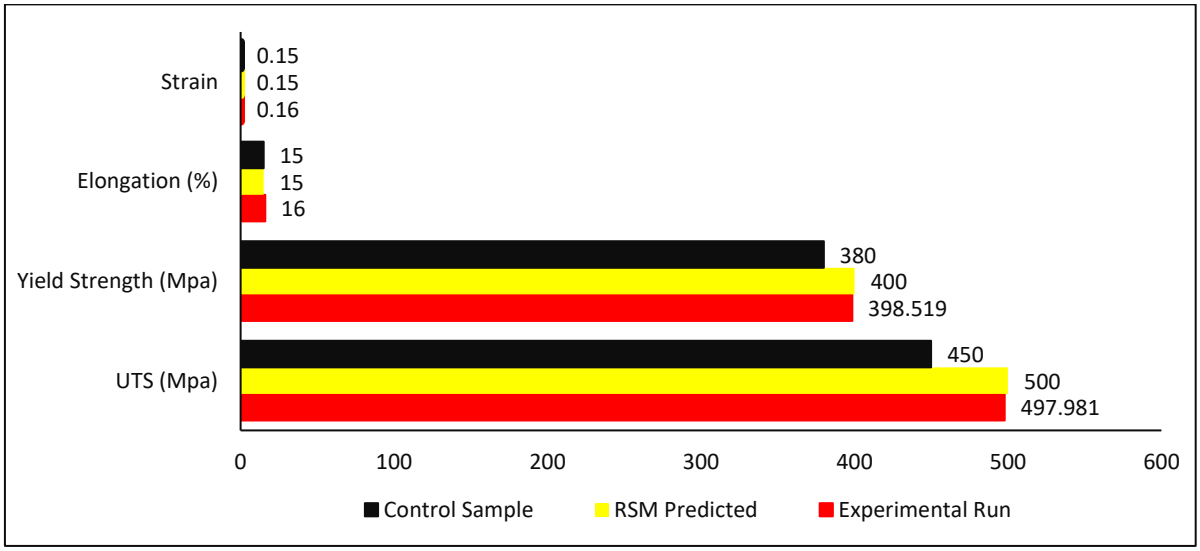

Figure 10: Plot of optimum welding process parameters with control sample, RSM predicted and welding run No. 8

In a study where AISI 4130 low carbon steel welded joint was examined, optimized predicted welding output parameters using Artificial Neural Network (ANN) were UTS of 421 and UTS of 427 MPa obtained from the experimental procedure. Optimized strain value of 0.61 obtained from ANN and strain of 0.62 obtained from the experimental procedure. Furthermore, optimized strain value of 61% was obtained using ANN while 62% elongation was obtained from the experimental process [11]. Disparities between the ANN predicted results and the experimental results for AISI 4130 and the results obtained in this study are not too outrageous and may be due to the material properties. For example, it was experimentally determined that UTS of AISI 1020 was 420 MPa, yield strength was 350 MPa and elongation was 36.5% [22]. Hence, the behavior and service performance of AISI related low carbon steel materials, may differ from one another depending on their carbon contents and alloying elements. In experimental study where the mechanical properties of AISI 1018 low carbon steel welded joint was examined, UTS of 440 MPa, yield strength of 370 MPa and elongation of 15% (0.15%) were obtained [23]. The UTS (450-500 MPa) obtained in this study was higher compared to UTS of 440 MPa in literature but closer to UTS value (450 MPa) obtained for the control sample in this study. The yield strength results (380-400 MPa) obtained in this study was higher compared to yield strength of 370 MPa in literature but closer to yield strength value (380 MPa) obtained for the control sample in this study. The results obtained for percentage elongation (0.15-0.16% MPa) in this study was within the percentage elongation of 0.15% in literature and correlated with the percentage elongation value (0.15%) obtained from RSM prediction and the control sample in this study. These results correlate slightly with the experimental determination of the mechanical properties of AISI 1018 [24], where UTS of 440, yield strength of 370MPa and elongation of 0.15% were obtained and UTS of 435, yield strength of 280MPa and elongation of 0.21% were obtained [25]. Results obtained from the aforementioned literature has to some extent shown moderate disparity when compared to the results obtained in this study. The

experimental, predicted and results obtained from control samples for UTS, yield strength, strain and percentage elongation can be used as a guide for studies conducted with similar material (AIS1 1018) and methods.

4. Conclusion

This study employed design expert in RSM to generate design of experiment for predicting pre-determined weld input variables (current, voltage, gas flow rate and welding speed) suitable for TIG welding experimental procedures and developing of numerical predictive models for optimum output responses (UTS, yield strength equivalent strain and percentage elongation). Twenty input welding runs were generated as design of experiment using Design Expert 7.01 software with the requirement to maximize UTS, yield strength and to minimize percentage elongation. The optimized input welding parameters required for optimum output response were applied experimentally in TIG welding process and numerically in RSM. The optimized welding parameters which fell under welding run No 8 were used as input for the TIG welding experiment and RSM prediction. Comparing the output results obtained from the control samples, welding experiment and RSM predicted values, significant correlations were observed in RSM predicted and experimentally determined welding results than those for the controlled samples. By increasing the gas flow rate with welding speed and voltage at moderate level, the values of UTS and yield strength were at maximum while strain and elongation were at minimum. An increase in current will only produce moderate UTS and yield strength while a moderate voltage and welding speed will always produce welded joint characterized by high UTS and yield strength with low strain and elongation. The UTS and yield strength of the welded joint were observed to be higher than those obtained from the parent metal (control sample), indicating that the weld joint was stronger than the parent metal. This may have been due to the interactions between the elemental constituent in the tungsten electrode and the constituents in the parent metal as well as the chemical and thermal reactions in the molten weld pool, thus, producing a stronger weld upon solidification.

Nomenclature

AISI	American iron and steel institute
ANN	Artificial neural network
ANOVA	Analysis of variance
CCD	Central composite design
DOE	Design of experiment
EDS	Energy dispersive spectroscopy
GTAW	Gas tungsten arc welding
HAZ	Heat affected zone
HRC	Hardness Rockwell
ISD	Induced stress distribution
RSM	Response surface methodology
SEM	Scanning electron microscopy
TIG	Tungsten inert gas
UTS	Ultimate tensile Strength
2FI	Two-factor integration
3D	Three dimension

References

[1] R. S. Parma (2010). Welding Engineering and Technology: 2nd Edition: New Delhi, Khanna Publishers, pp.18-353.
[2] K. S. Arun and S. Paulraj (2016). Multi-response optimization of process parameters for TIG welding of Incoloy 800HT by Taguchi grey relational analysis. Eng. Sci. and Tech., an Int. J. Vol.19(2), pp.811-817.
[3] R. A. Mohammed, M. Abdulwahab and E. T. Dauda (2013). Properties Evaluation of Shielded Metal Arc Welded Medium Carbon Steel Material. Int. J. of Inn. Res. in Sci, Eng and Tech. Vol.2(8), pp.3351-3357.
[4] A. E. Ikpe, I. Owunna and I. Ememobong (2017). Effects of Arc Voltage and Welding Current on the Arc Length of Tungsten Inert Gas Welding (TIG). Int. J. of Eng. Tech. Vol.3(4), pp.213-221.
[5] A. K. Srirangan and S. Paulraj (2016). Multi-response optimization of process parameters for TIG welding of Incoloy 800HT by Taguchi grey relational analysis. Eng. Sci. and Tech., an Int. J. Vol.19(2), pp.811-817.
[6] H. I. Kurt and R. Samur (2013). Study on Microstructure, Tensile Strength and Hardness 304 Stainless Steel Jointed by TIG Welding. Int. J. of Sci. and Tech. Vol.2(2), pp.163-168.
[7] A. G. Kamble and R. V. Rao (2013). Experimental Investigation on the Effects of Process Parameters of GMAW and Transient Thermal Analysis of AlSl 321 Steel. Adv. in Manf. Vol.1(4), pp.362-377.
[8] N. Sura and V. Mittal (2015). Experimental Study on Effects of Process Parameters on HAZ of Plain Carbon Steel Using GMAW. Int. J. of Latest Res. in Sci. and Techn. Vol.4(2), pp.167-170.
[9] O. D. Ikeh, A. E. Ikpe and V. Z. Njelle (2019). Effects of Electric Power Arc Inputs on the Fracture Surface and the Mechanical Properties of 0.4%C Steel. J. of Sci. and Techn. Res. Vol.1(3), pp.133-143.
[10] I. Owunna and A. E. Ikpe (2019). Finite Element Analysis of Tungsten Inert Gas Welding Temperatures on the Stress Profiles of AIS1 1020 Low Carbon Steel Plate. Int. J. of Eng. Tech. Vol.5(2), pp.50-58.
[11] I. B. Owunna and A. E. Ikpe (2019). Modelling and Prediction of the Mechanical Properties of TIG Welded Joint for AISI 4130 Low Carbon Steel Plates Using Artificial Neural Network (ANN) Approach. Nig. J. of Tech. Vol.38(1), pp.117-126.
[12] I. Owunna and A. E. Ikpe (2018). Optimization of TIG Welding Input Variables for AISI 1020 Low Carbon Steel Plate Using Response Surface Methodology. Int. J. of Eng. Sci. and App, Vol.2(3), pp.113-122.
[13] S. Bhattacharya (2021). Central Composite Design for Response Surface Methodology and Its Application in Pharmacy. Response Surface Methodology in Engineering Science, P. Kayaroganam, Intechopen Limited, London, United Kingdom.
[14] Prabhu, L., Kumar, S. S., Krishnamoorthi, S. and Prakash, S. (2019). Optimization of Vibration Parameters for Boring Bar Operation by RSM and ANN. Int. J. of Eng. and Adv, Tech, Vol.8(6), pp.2167-2176.
[15] A. Kumar and R. Gandhinathan (2020). Process Parameters for Metal Inert Gas Welding of Mild Steel by Using Taguchi Technique-A-Review. Int. J. of Mat. Sci and Tech, Vol.10(1), pp1-14.
[16] S. O. Sada (2018). Optimization of Weld Strength Properties of Tungsten Inert Gas Mild Steel Welds using the Response Surface Methodology. Nig. J. of Tech, 37(2), 407-415.
[17] L. M. Ebhota and C. E. Etin-Osa (2021). Prediction of Optimum Weld Tensile Strength Using Response Surface Methodology. Eur. J. of Eng. and Tech. Res, 6(3), 146-149.
[18] S. Nweze, J. Achebo and K. Obahiagbon (2019). Application of Response Surface Methodology in the Optimization and Prediction of Percentage (%) Weld Dilution of TIG Mild Steel Weldment. Int.J. of Sci. and Eng. Res, 10(1), 312-324.
[19] R. Gupta, K. Kumar and N. Sharma (2018). Multi-Performance Optimization in Friction Stir Welding of Aluminum Alloy Using Response Surface Methodology. Advances in Computational Intelligence and Robotics-Handbook of Research on Predictive Modelling and Optimization Methods in Science and Engineering, ISBN: 978152254, 240-263.
[20] S. Celik, A. D. Karaoglan and I. Ersozlu (2021). An Effective Approach Based on Response Surface Methodology for Predicting Friction Welding Parameters.
[21] S. Klitschke, A. Trondl and F. Huberth (2019). Influence of Strain Rate on Deformation and Failure Behaviour of Sheet Metals under Shear Loading. 12th European LS-DYNA Conference 2019, Koblenz, Germany.
[22] S. Dewangan, N. Mainwal, M. Khandelwal and P. Sunil (2019). Performance Analysis of Heat Treated AISI 1020 Steel Samples on the Basis of Various Destructive Mechanical Testing and Microstructural Behavior. Aus. J. of Mech. Eng, 1448, 1-14.
[23] K. D. Salman (2019). Microstructure and Mechanical Properties of Cold Roll AISI 1018 Low Carbon Steel. IOP Conf. Series: Mat. Sci and Eng. 551(012007), 1-5.
[24] A. Kumar, J. Kumar and R. Kumar (2015). Mechanical Properties and Structural Evolution during Warm Forging of Carbon Steel. Int. J. of Eng. Dev. and Res, 3(3), 1-10.
[25] A. Bhatia and R. Wattal (2021). Process Parameters Optimization for Maximizing Tensile Strength in Friction Stir-Welded Carbon Steel. Strojnisk Vestnik-J. of Mech. Eng, 67(6), 311-321.